

1 Titin Force is Enhanced in Actively Stretched Skeletal Muscle

2 Krysta Powers, Gudrun Schappacher-Tilp², Azim Jinha, Tim Leonard, Kiisa Nishikawa³ and
3 Walter Herzog

4 Human Performance Laboratory, Faculty of Kinesiology, University of Calgary

5 Department for Mathematics and Scientific Computing, NAWI Graz, Karl-Franzens-University
6 Graz²

7 Department of Biological Sciences, Northern Arizona University³

8 Corresponding Author: Walter Herzog

9 Human Performance Laboratory, KNB 404

10 2500 University Dr. NW

11 Calgary, AB Canada T2N 1N4

12 whertzog@ucalgary.ca

13

14 **ABSTRACT**

15 The sliding filament theory of muscle contraction is widely accepted as the means by
16 which muscles generate force during activation. Within the constraints of this theory, isometric,
17 steady-state force produced during muscle activation is proportional to the amount of filament
18 overlap. Previous studies from our laboratory demonstrated enhanced titin-based force in
19 myofibrils that were actively stretched to lengths which exceeded filament overlap. This
20 observation cannot be explained by the sliding filament theory. The aim of the present study was
21 to further investigate the enhanced state of titin during active stretch. Specifically, we confirm
22 that this enhanced state of force is observed in a mouse model and quantify the contribution of
23 calcium to this force. Titin-based force was increased by up to four times that of passive force
24 during active stretch of isolated myofibrils. Enhanced titin-based force has now been
25 demonstrated in two distinct animal models, suggesting that modulation of titin-based force
26 during active stretch is an inherent property of skeletal muscle. Our results also demonstrated
27 that 15% of titin's enhanced state can be attributed to direct calcium effects on the protein,
28 presumably a stiffening of the protein upon calcium binding to the E-rich region of the PEVK
29 segment and selected Ig domain segments. We suggest that the remaining unexplained 85% of
30 this extra force results from titin binding to the thin filament. With this enhanced force confirmed
31 in the mouse model, future studies will aim to elucidate the proposed titin-thin filament
32 interaction in actively stretched sarcomeres.

33

34

35

36

37

38

39 Keywords: titin, skeletal muscle, force enhancement, cross-bridge theory, eccentric contractions

40 INTRODUCTION

41 The current, and generally accepted, theory which explains active force production in
42 muscle is the sliding filament-based cross-bridge model. This model predicts that active force is
43 produced when cross-bridges cyclically form between the thick and thin filaments in the
44 sarcomere (Huxley and Simmons, 1971). Therefore, for a given level of activation, the isometric
45 steady-state force generated by an active muscle should be proportional to the number of cross-
46 bridges that can form, which corresponds to the amount of overlap between the thick and thin
47 filaments (Gordon et al., 1966; Huxley and Niedergerke, 1954). This constitutes the force-
48 sarcomere length relationship, which is generally adhered to during isometric contractions
49 (Gordon et al., 1966). However, following eccentric, or lengthening, contractions the isometric
50 steady-state force produced at a given sarcomere length exceeds the predictions of the force-
51 length relationship (Abbot and Aubert, 1952; Edman et al., 1978; Edman et al., 1982; Herzog et
52 al., 2006; Leonard and Herzog, 2010; Morgan, 1994). This property, termed residual force
53 enhancement, provides a direct challenge to the sliding filament-based cross-bridge theory.

54 Residual force enhancement has been observed *in vivo* and down to the sarcomere level
55 (Abbott and Aubert, 1952; Edman et al., 1982; Herzog and Leonard, 2002; Leonard et al., 2010;
56 Rassier, 2012). There are three main filaments at the sarcomere level that contribute to force
57 production in muscle: the thick (myosin), the thin (actin), and the titin filaments. The thick
58 filament is comprised primarily of the protein myosin and the thin filament is comprised of actin
59 and regulatory proteins. Interactions between the thick and thin filaments are understood to
60 generate active force during muscle contraction. Titin is a spring-like protein that produces
61 passive force when sarcomeres are stretched beyond a certain resting length. With increased
62 stretch on the descending limb of the force-sarcomere length relationship, the contribution of
63 titin to the total force produced increases exponentially (Granzier and Labeit, 2004). In an
64 attempt to explain how sarcomeres can produce force beyond what is provided by the
65 interactions between thick and thin filaments, it has been suggested that residual force
66 enhancement may be the result of a passive element becoming ‘engaged’ during active stretch
67 (Edman et al., 1982; Forcinito et al., 1998; Herzog and Leonard, 2002; Herzog et al., 2012a;
68 Herzog et al., 2012c; Monroy et al., 2012; Nishikawa et al., 2012). Residual force enhancement
69 exhibits properties that allude to a passive force contribution in the sarcomere. Residual force

70 enhancement increases with increased magnitude of stretch and is greater as the muscle is
71 stretched further on the descending limb of the force-length relationship (Edman et al., 1982).
72 Additional studies have observed enhanced passive force in muscles following active stretch
73 (Herzog and Leonard, 2002; Joumaa et al., 2008; Labeit et al., 2003), alluding to a passive
74 element in the property of force enhancement

75 Titin is the primary contributor to passive force at the myofibrillar level (Wang et al.,
76 1991). Titin is a dynamic protein that contributes to many different aspects of muscle function,
77 including passive force production (28), myofibrillar assembly (Gregorio et al., 1999), centering
78 of the thick filament (Horowitz and Podolsky, 1987), sarcomere stability (Herzog et al., 2012c),
79 and various signaling events (Granzier and Labeit, 2004). Titin is functionally separated into a
80 structural A-band and an extensible I-band region (Fig. 1). Titin's I-band region is comprised of
81 a proximal Ig and PEVK spring, linked by the N2A segment (Wang et al., 1991). The distal Ig
82 domain connects the segment to the A-band. During stretch, elongation of titin's I-band,
83 particularly the PEVK segment, produces force (Gautel and Goulding, 1996). The spring
84 properties of I-band titin can be rapidly adjusted in response to mechanical demands on the
85 sarcomere (Granzier and Labeit, 2004). Phosphorylation (Hidalgo et al., 2009; Krüger et al.,
86 2009), small heat shock protein infiltration (Kötter et al., 2014) and disulfide bonding (Alegre-
87 Cebollada et al., 2014) are among the many processes by which the stiffness of I-band titin can
88 be modulated to protect the protein from damage during stretch. While the contribution of titin-
89 based stiffness to muscle force has traditionally been limited to passive stretch, this conventional
90 view of titin is now being challenged with numerous studies which also demonstrate tuning of
91 titin's spring properties during calcium activation (Bianco et al., 2007; Campbell and Moss,
92 2002; Labeit et al., 2003; Leonard and Herzog, 2010; Monroy et al., 2007; Tatsumi et al., 2001).
93 The configuration of titin's extensible I-band is changed in the presence of calcium (Tatsumi et
94 al., 2001). Specifically, it has been shown that the stiffness of titin's I-band region increases
95 when calcium ions bind to the PEVK region and Ig domains (DuVall et al., 2013; Labeit et al.,
96 2003). In addition to intrinsic changes to the stiffness of titin, calcium-dependent interactions
97 between titin and the thin filament have also been observed (Kellermayer and Granzier, 1996).
98 These observations support the speculation that titin may be engaged during active stretch
99 (Edman et al., 1982; Herzog et al., 2006; Herzog et al., 2012a; Herzog et al., 2012c; Leonard and
100 Herzog, 2010; Nishikawa et al., 2012).

101 Recently, Leonard and Herzog (2010) investigated modulation of titin-based force during
102 active stretch beyond filament overlap. The findings of that study indicated that the increase in
103 titin-based stiffness must employ an additional mechanism other than calcium to produce the
104 increase in force that was observed since no effect of calcium activation, in the absence of cross-
105 bridge-based active forces, was observed. They speculated that modulation of titin-based force
106 may occur when titin binds to the thin filament during strong cross-bridge binding to actin
107 (Leonard and Herzog, 2010). While titin binding to the thin filament has been previously
108 suggested (Edman et al., 1982; Herzog et al., 2006; Leonard and Herzog, 2010; Nishikawa et al.,
109 2012), a mechanism by which this may occur remains to be discovered.

110 Recent experiments (Monroy et al., 2012; Nishikawa et al., 2012) using muscles from
111 mice with a mutated titin protein may provide insight into the region of titin that modulates titin-
112 based stiffness during active stretch. The muscular dystrophy with myositis (*mdm*) model is a
113 genetic mutation in the mouse genome which results in a deletion of amino acids from the N2A
114 region of titin (Garvey et al., 2002). The deletion of a predicted 83 amino acids from distal N2A
115 (9 of which are deleted from proximal PEVK) results in progressive degeneration of skeletal
116 muscle in mice (Garvey et al., 2002). This is a modest deletion considering the ~33,000 amino
117 acids encompassing the titin protein. Nevertheless, the *mdm* deletion has profound effects on the
118 musculoskeletal system of mice (Garvey et al., 2002; Huebsch et al., 2005). Despite the visible
119 differences in phenotype between *mdm* and wild-type mice, it remains unclear how the *mdm*
120 mutation affects titin functionally. However, whole muscle experiments demonstrate that
121 modulation of titin-based stiffness does not occur in *mdm* soleus during calcium activation
122 (Nishikawa et al., 2012), thereby suggesting the possibility that modulation of titin-based force
123 occurs within the deleted region of *mdm* titin. We would like to investigate this possibility.
124 However, prior to embarking on such experiments, the properties of titin-based force
125 enhancement in actively stretched muscles need to be confirmed in the mouse model, and the
126 contribution of calcium activation in the absence of cross-bridge-based active forces on titin's
127 stiffness and force need to be carefully determined.

128 The purpose of this study was to determine whether modulation of titin-based force
129 during active stretch occurs in the wild-type, or normal, mouse and to quantify the effects of
130 calcium activation on titin stiffness to further elucidate the mechanism of titin-based force

131 enhancement during active stretch. Enhanced titin-based force with active stretch has only been
132 directly observed in experiments using rabbit psoas myofibrils (Leonard and Herzog, 2010) and
133 needs to be confirmed in another animal model, as was previously suggested (Granzier, 2010). In
134 addition, the experiments by Leonard & Herzog were unable to resolve an effect of calcium on
135 the increase in stiffness of titin, possibly due to the high variation of their data. This is surprising
136 as calcium has been shown to increase the stiffness of titin (DuVall et al., 2013; Joumaa et al.,
137 2008; Labeit et al., 2003). Thus, this study specifically aimed to quantify the contribution of
138 calcium effects to titin's enhanced force. We hypothesized that titin-based stiffness would be
139 increased in actively stretched mouse skeletal muscle and that the increase in stiffness would not
140 be explained entirely by the effects of calcium on titin stiffness.

141 **RESULTS**

142 The steady state force following stretch was greater in active than passive experiments
143 (Fig. 3A). Individual sarcomere lengths were measured at the end of stretch in a subset of three
144 active and three passive experiments to ensure that filament overlap was lost in all sarcomeres.
145 Although sarcomere length non-uniformities were present, all measured sarcomeres were beyond
146 filament overlap at the end of stretch (Fig. 3B) (average sarcomere length 6.0 μm). The shortest
147 sarcomeres measured in active and passive myofibrils stretched to an average sarcomere length
148 of 6.0 μm were 4.15 μm and 4.07 μm respectively.

149 Calcium activated myofibrils produced more force during stretch compared to passive,
150 cross-bridge inhibited (BDM), and TnC-depleted myofibrils at all measured sarcomere lengths
151 (2.5-6.0 μm) ($p < 0.01$) (Fig. 4). Therefore, calcium activated myofibrils produced more force
152 both within the region of filament overlap ($< 4.0 \mu\text{m}$) and beyond the region of thick-thin
153 filament overlap (~ 4.0 -6.0 μm) in mouse psoas myofibrils that were either not activated, or were
154 activated but force production was prevented, either by depletion of a regulatory protein (TnC)
155 or by inhibiting strong cross-bridge binding (BDM).

156 BDM treated and TnC-depleted myofibrils produced significantly less force than calcium
157 activated myofibrils at all sarcomere lengths ($p < 0.01$). However, they produced more force than
158 the passively stretched myofibrils across all sarcomere lengths exceeding 3.5 μm ($p < 0.05$) (Fig.
159 4). For sarcomere lengths beyond myofilament overlap, the force increase in BDM treated and
160 TnC-depleted myofibrils averaged approximately 15% of the total increase observed in the

161 normal (non-inhibited) myofibrils. BDM treated and TnC-depleted myofibrils did not differ in
162 force at any sarcomere lengths.

163 Simulations using a three-filament model (Schappacher-Tilp et al., *submitted* 2014)
164 assumed that titin's N2A region binds to the thin filament leaving only the PEVK region and the
165 distal Ig domains as free spring elements (Fig.5). Forces predicted in actively stretched
166 sarcomeres with N2A thin-filament binding exceeded passive force predictions. Forces predicted
167 for actively stretched sarcomeres without N2A thin-filament binding were deficient in titin-based
168 force enhancement. There was a small increase in predicted force between actively (without N2A
169 thin-filament binding) and passively stretched myofibrils (~12%). Predicted force-elongation
170 curves of actively stretched sarcomeres without N2A thin-filament binding closely resembled
171 TnC-depleted and BDM treated experimental observations.

172 **DISCUSSION**

173 The first aim of this study was to determine whether titin-based force is increased during
174 active compared to passive stretch of mouse skeletal muscle myofibrils. Previous experiments in
175 rabbit psoas myofibrils showed that at lengths beyond filament overlap, titin-based force is much
176 greater in active compared to passive stretching. The increase in titin-based force from these
177 studies could not be explained with any known mechanism of sarcomere force modulation
178 (Leonard and Herzog, 2010). The results from the present study demonstrate that titin-based
179 force is also greater during active compared to passive stretch in mouse psoas myofibrils. This
180 modulation of titin force allows the sarcomere to maintain its force-generating capability during
181 active stretch to lengths beyond filament overlap and provides a protective mechanism within the
182 sarcomere by which active stretch is limited.

183 In actively stretched mouse psoas myofibrils, forces exceeded the force observed in
184 passively stretched myofibrils matched at all sarcomere lengths. One would expect that at
185 sarcomere lengths within filament overlap ($< 4.0 \mu\text{m}$), calcium activated myofibrils produce
186 more force than non-activated myofibrils because of the active forces produced by cross-bridge
187 interactions between the contractile filaments actin and myosin. However, cross-bridge forces
188 cannot be used to explain the increase of force production in calcium activated myofibrils that
189 are stretched beyond filament overlap ($> 4.0 \mu\text{m}$) (Leonard and Herzog, 2010). At these lengths,

190 cross-bridges cannot form and titin is virtually the exclusive contributor to myofibril force
191 (Herzog et al., 2012b).

192 It is well-known that sarcomeres in muscles (Llewellyn et al., 2008), fibers (Page and
193 Huxley, 1963) and myofibrils (Panchangam and Herzog, 2011; Panchangam and Herzog, 2012)
194 are non-uniform in lengths. Despite this non-uniformity, all individual sarcomeres measured in
195 selected experiments were stretched beyond actin-myosin filament overlap (4.0 μm) in our active
196 and passive stretch tests. Therefore, we feel confident that most sarcomeres and half-sarcomeres
197 could not produce any active, cross-bridge based force once the final stretch length was reached.
198 If some sarcomeres or half-sarcomeres still had overlap between actin and myosin filaments, this
199 non-uniformity could not explain the four times higher forces observed in actively stretched
200 myofibrils at the final length (6.0 μm /sarcomere) compared to the passively stretched myofibrils,
201 and it definitely could not explain the four times higher forces compared to the active forces
202 obtained when the average sarcomere length was optimal (active stretch, 2.5 μm /sarcomere; Fig.
203 4). The reason for this assertion is that a myofibril, by definition, consists of serially arranged
204 sarcomeres. From a mechanical point of view, that means that each half-sarcomere and
205 sarcomere must transmit exactly the same force as all other (half-) sarcomeres, and this force
206 transmission is limited by the weakest half-sarcomere. Thus, independent of whether a single or
207 half-sarcomere maintains some remnant myofilament overlap, it could not explain the results
208 observed here. A completely different mechanism than myofilament overlap or sarcomere length
209 non-uniformity must be at work.

210 In the presence of calcium, titin-based stiffness increases (DuVall et al., 2013; Labeit et
211 al., 2003). This calcium initiated increase in titin-based stiffness was a likely contributor to the
212 enhanced titin force observed during active stretch of myofibrils. Therefore, with confirmation
213 that titin-based force was enhanced during active stretch in the mouse, subsequent experiments
214 sought to quantify the contribution of calcium to titin's enhanced state. Experiments using BDM
215 and TnC-depletion were conducted to potentially identify the mechanisms underlying the
216 observed increase in titin-based stiffness in actively stretched myofibrils. TnC-depleted
217 myofibrils can be calcium activated but produce no active force as calcium binding to the
218 regulatory TnC protein is not possible, thus the binding site of the cross-bridge on actin remains
219 inaccessible to cross-bridges (Moss et al., 1985). Similarly, BDM treated myofibrils can be

220 calcium activated, and allow for cross-bridge binding to actin in the weakly bound state, but
221 BDM prevents phosphate release from the nucleotide pocket of the cross-bridge, thereby
222 inhibiting strong cross-bridge binding (Tesi et al., 2002). At sarcomere lengths beyond
223 myofilament overlap (4.0-6.0 μm), calcium activation in BDM treated and TnC-depleted
224 myofibrils increased titin force by approximately 15% of the total increase observed in actively
225 (but non-force inhibited) compared to passively stretched myofibrils. Therefore, it appears that
226 although calcium activation provides increased stiffness to titin, and thus increased force upon
227 sarcomere stretching, this effect is minimal. The full amount of increased titin-based force,
228 which we will refer to as “titin-based force enhancement” requires active force production and
229 strong cross-bridge binding to actin.

230 Interestingly, the myofibril forces in BDM treated and TnC-depleted myofibrils were the
231 same when sarcomeres were stretched beyond filament overlap. In TnC-depleted myofibrils,
232 there is thought to be no cross-bridge attachment to actin, and titin-enhancement is small, as
233 shown above. In BDM treated myofibrils, weak cross-bridge binding is thought to occur, and
234 small configurational changes in the regulatory proteins troponin and tropomyosin would be
235 expected, but even these events do not produce titin force beyond that observed in the TnC-
236 depleted myofibrils. Thus, weak cross-bridge binding and some configurational changes in the
237 regulatory proteins do not seem sufficient to allow for the full titin-based force enhancement
238 observed in intact, non-inhibited actively stretched myofibrils.

239 If calcium activation alone is not sufficient to explain the increase in titin stiffness during
240 active stretch, an additional mechanism by which titin-based force is enhanced during active
241 stretch must be at work. Of the various known mechanisms by which titin-based stiffness can be
242 rapidly and reversibly adjusted, we are currently unaware of any mechanism by which titin
243 stiffness is increased by up to 400%. Therefore, we are of the impression that the titin spring
244 must become shorter in actively stretched sarcomeres to explain our findings. It was recently
245 hypothesized that titin-based force may be enhanced when cycling cross-bridges both translate
246 and rotate the thin filaments, winding titin upon the thin filament during activation (Nishikawa et
247 al., 2012). While logistically discreet, this hypothesis conceptually aligns with our assumption
248 that the available spring length of titin must decrease in actively stretched sarcomeres.
249 Shortening of the titin spring could occur by any number of mechanisms. However, the simplest

250 way to explain titin-based force enhancement is by assuming that titin binds to the thin filament
251 when cross-bridges bind strongly to the thin filament. Thin-filament-titin interactions are well
252 documented in cardiac muscle (Kellermayer and Granzier, 1996), however, much less is known
253 concerning the interaction between skeletal muscle titin and the thin filament. We acknowledge
254 the vast possibilities by which titin-thin filament interactions could increase the stiffness of titin
255 and the precise location and characteristics of this mechanism will require further investigations.

256 We previously proposed that a binding site for titin on the thin filament may be exposed
257 during the movement of regulatory proteins with the influx of calcium (Herzog et al., 2012a;
258 Herzog et al., 2012c; Leonard and Herzog, 2010). However, the results from the present study
259 suggest that movement of regulatory proteins is not sufficient to initiate titin-based force
260 enhancement. This is because there was no difference in force between TnC-depleted myofibrils
261 (no movement of regulatory proteins) and BDM treated myofibrils (presumed movement of
262 regulatory proteins). Therefore, we now speculate that with the influx of calcium and the
263 initiation of cross-bridge cycling, one (or many) site(s) on the thin filament are exposed,
264 allowing titin-thin filament binding to decrease the available spring length of titin in an activated
265 sarcomere (Fig. 6). This hypothesis is particularly attractive as it provides an energetically
266 efficient and reversible mechanism by which titin-based force could be modulated during
267 activation. Experimental support for titin-thin filament interactions is provided by experiments in
268 rabbit longissimus dorsi muscle, which demonstrate calcium-dependent changes in titin-actin
269 interactions. In these studies an unidentified segment of titin demonstrated binding to actin
270 filaments in a calcium-dependent manner (Kellermayer and Granzier, 1996). While this segment
271 of titin has not been identified, these results provide support for the idea that titin may bind to the
272 thin filament during calcium-activation.

273 Recent speculation that the N2A segment of titin may be the site of thin filament-titin
274 binding (Nishikawa et al., 2012) provides the basis for a focused investigation. The N2A
275 segment of titin has a mechanical role in passive skeletal muscle, resisting stretch at long
276 sarcomere lengths (Granzier and Labeit, 2004) and is also a main player in numerous skeletal
277 muscle signaling events (Huebsch et al., 2005). Binding at the N2A segment of titin would be
278 mechanically advantageous as it would prevent the proximal Ig domain from extending upon
279 stretch (Fig. 6) and allow the high-force PEVK region to be recruited immediately upon stretch

280 (Nishikawa et al., 2012). The hypothesis that N2A titin is the site of titin-thin filament binding is
281 based on studies in the *mdm* mouse model, which is characterized by a deletion in the N2A
282 region of titin (Garvey et al., 2002). During active unloading of whole mouse soleus muscles, the
283 titin spring is shorter and stiffer than in passive soleus muscles while no change in length or
284 stiffness is observed in soleus muscles of *mdm* mice during active unloading (Monroy et al.,
285 2012). These results suggest that the mechanism by which titin achieves an enhanced state of
286 stiffness during calcium activation is altered in *mdm* titin. Further support for N2A as the site of
287 titin-thin filament binding is provided by reports that suggest a fundamental difference in titin-
288 actin interactions between skeletal muscle that expresses N2A titin and cardiac muscle that
289 expresses N2B (Yamasaki et al., 2001).

290 To investigate this hypothesis further, we modeled the proposed N2A titin-thin filament
291 interaction to determine whether this mechanism could explain titin-based force enhancement.
292 We assumed that titin's N2A region binds to the thin filament leaving only the PEVK region and
293 the distal Ig domains as free spring elements. While the predicted absolute values of stress based
294 on the rabbit psoas model differ from the experimental results from mouse, we can study the
295 impact of N2A-thin filament binding on force predictions conceptually (Fig. 5). Forces predicted
296 during actively stretched sarcomeres with N2A thin-filament binding show a substantial force
297 gain at long sarcomere lengths vastly exceeding purely passive forces and forces predicted for
298 activation without N2A binding. With N2A-thin filament binding, titin-based force predicted by
299 the model was doubled in actively stretched sarcomeres. Experimental results demonstrate 3-4
300 times greater titin-based force in actively stretched mouse psoas myofibrils and approximately 3
301 times greater in rabbit psoas myofibrils (Leonard and Herzog, 2010) which exceeds the force
302 predicted by the model. By shifting the binding site on titin towards the M-line, the force gain
303 would be substantially higher; suggesting that the binding site on titin would be located at or
304 distal to the N2A segment. When simulations were performed in the absence of N2A-thin
305 filament binding, the model predictions of titin-based force coincided closely with cross-bridge
306 inhibited (TnC-depleted and BDM) sarcomeres, which were deficient in titin-based force
307 enhancement (Fig. 4). The predicted force of actively stretched myofibrils without titin binding
308 still exceeded passive forces, presumably due the binding of calcium to the PEVK and Ig
309 domains (DuVall et al., 2013; Joumaa et al., 2008; Labeit et al., 2003; Ting et al., 2012), but only
310 to a small extent. Overall, these simulations conceptually reflect the experimental results and

311 proposed mechanism that titin is bound to the thin filament during activation. To reproduce the
312 absolute values of the experimental results one might need to fit the parameters for the mouse
313 model. Nevertheless, the conceptual premise of the results observed in mouse myofibrils
314 supports titin binding to the thin filament at or distal to the N2A segment.

315 With the enhanced force of titin confirmed in the mouse skeletal muscle, future
316 experiments can utilize the *mdm* model to further investigate the role of N2A titin in titin-based
317 force enhancement. In a preliminary investigation, we isolated and stretched calcium activated
318 and non-activated *mdm* myofibrils using the same experimental protocol described below to
319 determine whether the *mdm* deletion in N2A titin affects titin-based force enhancement. Isolated
320 *mdm* myofibrils did not differ in diameter or structure and thus were expected to contain the
321 same quantity of contractile material and force-producing capability as in wild-type myofibrils.
322 Despite our expectations, when activated at the plateau of the force-length relationship,
323 contraction force was decreased in *mdm* compared to wild-type myofibrils activated at
324 corresponding sarcomere lengths. During active stretch, titin-based force enhancement was
325 present in *mdm* (Fig. 7) but to a much lesser extent than in actively stretched wild-type
326 myofibrils (Fig 4), suggesting that titin-based force enhancement is affected by the *mdm*
327 deletion. These pilot results are in accordance with the proposed mechanism that N2A titin binds
328 to the thin filament to achieve enhanced force during active stretch; however, additional
329 experiments and considerations are required in the interpretation of these results. Whether N2A
330 is the site of titin that binds to the thin filament during calcium activation will require a more
331 focused investigation. Nevertheless, this preliminary data is a strong indication that N2A titin is
332 a binding site or otherwise involved in the mechanism of titin-based force enhancement.

333 When considering an interaction between titin and the thin filament in explaining
334 enhanced titin-based force during active stretch, it is important to consider that with the
335 exception of calcium stiffening of titin, titin-based force enhancement was abolished when
336 strong cross-bridge cycling was inhibited. This result suggests that titin's enhanced state is at
337 least in part dependent on the presence of cross-bridge cycling and active force. Previous results
338 from rabbit psoas myofibrils showed that titin-based force enhancement was decreased when the
339 myofibril was activated at long sarcomere lengths, with less than optimal filament overlap
340 (Leonard and Herzog, 2010). If titin-thin filament interactions are partially responsible for the

341 enhancement of titin-based force, these results would suggest that the interaction occurs with the
342 onset of cross-bridge cycling, and thus, at sarcomere lengths where initial activation occurs. This
343 indicates that titin's contribution to the force produced during active stretch spans the full length
344 of stretch. While the present study could not disseminate any contribution of titin to active force
345 within the region of overlap, the question of whether titin contributes to the force generated
346 within the region of overlap during active stretch is an important topic for future studies.

347 When considering the property of titin-based force enhancement within the context of an
348 intact muscle fiber it is important to consider the various additional structures which provide
349 resistive forces to protect the sarcomeres (and titin) from potentially hazardous elongation.
350 Within working muscle fiber lengths, titin and collagen are the main contributors to passive force
351 (Granzier and Irving, 1995). Individual sarcomeres are also surrounded by a network of
352 intermediate filaments which resist sarcomere stretch to lengths that cause structural damage
353 ($>4.5 \mu\text{m}$) (Wang et al., 1993). At these long sarcomere lengths, the intermediate filament
354 network acts as a force-bearing structure, contributing about one quarter of the total passive force
355 (Wang et al., 1993). In the absence of resistive forces provided by collagen and intermediate
356 filaments, which are integral in providing protection against stretch-induced sarcomere injury,
357 our results refer only to titin-based mechanics in the sarcomere. As residual force enhancement
358 has been observed at the single sarcomere level (Leonard et al., 2010; Rassier, 2012), these
359 experiments were designed to specifically address titin-based force enhancement in the actively
360 stretched intact sarcomeres. While intermediate filaments, collagen and additional structures also
361 contribute to the resistive force limiting sarcomere stretch within a muscle fiber, our results
362 indicate that titin-based force enhancement is a fundamental mechanical property of the
363 sarcomeres themselves, which provides an inherent resistance to actively stretching sarcomeres.

364 In summary, we found that titin-based force is increased in actively stretched mouse
365 psoas myofibrils at lengths beyond filament overlap. With studies from rabbit and mouse
366 demonstrating this property, we propose that enhanced titin-based force beyond the effects of
367 calcium is an inherent property of actively stretched skeletal muscle. Calcium activation alone
368 could only explain 15% of the increase in titin-based force beyond filament overlap; therefore we
369 propose that with the onset of cross-bridge cycling and active force, titin binds to the thin
370 filament and decreases its available spring length resulting in a drastic increase in its spring

371 stiffness. This mechanism would provide the sarcomere with an additional source of force
372 production during active stretch, which could potentially provide an explanation for how
373 skeletal muscles achieve enhanced force following active stretch. While additional experiments
374 are needed to elucidate the mechanism by which titin-based force enhancement occurs, our
375 results suggest that it is initiated when a site on titin (at or distal to the N2A segment) binds to
376 the thin filament with the onset of cross-bridge cycling. With past and present studies
377 demonstrating a role for titin in active muscle, our understanding of force production should
378 begin to expand the contribution of titin in actively stretched skeletal muscle.

379 **MATERIALS AND METHODS**

380 *Sample Preparations*

381 A myofibril is the smallest structural unit of muscle that maintains the natural
382 architecture of the contractile apparatus (Yang et al., 1998). In a single myofibril, extracellular
383 connective tissues are absent and all force measured must be generated by the proteins
384 comprising sarcomeres in series. Therefore, myofibril experiments are ideal for the investigation
385 of the contribution of titin to force production in sarcomeres as described previously (Leonard
386 and Herzog, 2010).

387 *Experiment setup*

388 All tests were conducted using an inverted microscope (Zeiss Axiovert 200M) equipped
389 with a $\times 100$ oil immersion objective (numerical aperture 1.3) with a $\times 2.5$ Optovar (Leonard and
390 Herzog, 2010) under $\times 100$ oil immersion.

391 Myofibril forces were determined using custom-built nanofabricated silicon nitride
392 cantilevers with two arms and a stiffness of 21 or 68 pN/nm (Fig. 2). Myofibrils were glued
393 (Dow Corning 3145) to one of the lever arms at one end and wrapped around a stiff glass needle
394 at the other end. Displacement of one cantilever arm attached to the myofibril relative to the
395 second reference arm was measured using a custom MATLAB program. Force was calculated
396 from the measured displacement and the known lever stiffness and expressed in units of stress
397 ($\text{nN}/\mu\text{m}^2$) by normalizing the measured force to the cross-sectional area of each myofibril.

398 *Materials*

399 Strips of mouse psoas muscle were extracted from euthanized animals and tied to wooden
400 strips to preserve the *in situ* length. The muscle strips were placed in a rigor-glycerol solution (-
401 20°C, pH 7.0) with protease inhibitors (Complete®, Roche Diagnostics, Montreal, QB, Canada)
402 and stored at -20°C for 12-17 days (Leonard and Herzog, 2010). For experiments, muscle strips
403 were homogenized in a rigor solution at 4°C and tested at 20°C (Leonard and Herzog, 2010).
404 Activation of myofibrils was achieved by direct application of calcium ions in an activation
405 solution (pCa 3.5) (Leonard and Herzog, 2010). Ethics approval was granted by the Life and
406 Environmental Sciences Animal Ethics Committee of the University of Calgary.

407 *Experimental Protocol*

408 Single myofibrils with four to twelve sarcomeres in series were mounted between a
409 needle for controlled length changes and a cantilever to measure force (Fig. 3). Myofibril lengths
410 were adjusted to an initial average sarcomere length of 2.5 μm . Previous experiments
411 demonstrated a force-dependent component to titin-based enhanced force (Leonard and Herzog,
412 2010). Therefore, to maximize the magnitude of titin-based force enhancement in the present
413 study, myofibrils were activated slightly above the plateau region and then stretched. The thin
414 filament length in mouse psoas is $\sim 1.11 \mu\text{m}$ (Bang et al., 2009; Burkholder and Lieber, 2001)
415 and myofilament overlap in mouse psoas would be expected to be lost at sarcomere lengths of
416 approximately 3.95 μm (Herzog et al., 1992). Therefore, when the average sarcomere lengths
417 within a myofibril exceed 4.0 μm , we can safely assume that some sarcomeres and half-
418 sarcomeres are pulled beyond myofilament overlap, and thus their forces, which are strictly in
419 series with the rest of the myofibril, have to match those produced in the remaining sarcomeres.
420 Individual sarcomere lengths were measured at the end of stretch to confirm the loss of filament
421 overlap.

422 Average sarcomere lengths were determined by dividing the total length of the myofibril
423 by the number of sarcomeres. All myofibrils were stretched from an average sarcomere length of
424 approximately 2.5 μm to lengths of approximately 6.0 μm , thereby achieving lengths that far
425 exceeded filament overlap. Stretching was applied at a speed of 0.1 μm per sarcomere per
426 second. After stretch, myofibrils were held isometrically until a steady-state force was reached.

427 The inclusion criterion for successful myofibril experiments were determined and strictly
428 adhered to. A myofibril experiment was considered successful if (1) all sarcomeres lengthened
429 and (2) the force increased with stretch for the entire duration of stretch. In actively stretched
430 myofibril experiments, in addition to the two criteria stated above, all sarcomeres had to visibly
431 shorten upon activation for the experiment to be considered viable. All experiments which did
432 not exhibit the established criterion were excluded from statistical analyses.

433 *Experimental Groups*

434 *Group 1 – passive:* myofibrils (n = 10) were passively stretched in a non-activating (pCa
435 = 8.0) solution containing ATP. This group demonstrates the mechanical properties of the
436 passive titin spring.

437 *Group 2 – active:* myofibrils (n = 7) were activated in a calcium-ATP (pCa 3.5)
438 activation solution and then stretched. Active, actin-myosin-based cross-bridge forces cease to
439 exist at sarcomere lengths beyond myofilament overlap (i.e., ~4.0 μm) (Gordon et al., 1966;
440 Huxley, 1957; Leonard and Herzog, 2010).

441 *Group 3 – TnC depleted:* myofibrils (n = 8) were incubated in a low ionic strength rigor-
442 EDTA solution (pH 7.8) for 10 minutes to inhibit cross-bridge formation by depletion of
443 Troponin C (TnC) (Joumaa et al., 2008) and then stretched in calcium-ATP activation solution.
444 The TnC-depletion protocol used in this study has been described previously and its
445 effectiveness in eliminating TnC from actin, thereby preventing any cross-bridge based forces,
446 has been verified using gel electrophoresis and force measurements, respectively (Joumaa et al.,
447 2008).

448 *Group 4 – BDM:* myofibrils (n = 8) were stretched in a calcium-ATP activation solution
449 with 20nM butanedione monoxime (BDM), an inhibitor of strong cross-bridge binding to actin
450 (Tesi et al., 2002). All solutions used in this study have been previously published (Joumaa et al.,
451 2008; Leonard and Herzog, 2010).

452 *Modeling*

453 The proposed N2A titin-thin filament interaction was simulated to determine whether it
454 could explain titin-based force enhancement in previous (Leonard and Herzog, 2010) and present

455 observations. A detailed description of the mathematical model is provided elsewhere
456 (Schappacher-Tilp et al., *submitted* 2014). Briefly, the simulations consider active force
457 production based on a five-state cross-bridge model (Piazzesi and Lombardi, 1995; Rayment et
458 al., 1993) and passive force production based on elongation of titin. In the case of actin-titin
459 binding upon activation, we assume that titin's N2A region binds to the virtually rigid thin
460 filament thereby reducing titin's free spring length. The binding between actin and titin does not
461 generate force but directly influences passive force generation. The total force exerted by a
462 sarcomere is given by the sum of cross-bridge based active force and variable titin-based passive
463 force. The latter is calculated by Monte Carlo simulations performed for 200 titin strands, and
464 normalized to the passive forces in a sarcomere of $1\mu\text{m}^2$ cross sectional area. In order to
465 eliminate any bias toward the titin-thin filament binding model, we refrained from fitting the
466 experimental data, but rather used well known model parameters from the literature based on
467 rabbit psoas titin (Linke et al., 1998; Linke et al., 2002; Prado et al., 2005). The model
468 predictions were scaled to experimental mouse psoas values and expressed as predicted stress
469 ($\text{nN}/\mu\text{m}^2$) by average sarcomere length (μm)

470 *Statistical Analysis*

471 A Kruskal Wallis non-parametric ANOVA was performed and followed-up with a Mann-
472 Whitney U group-wise comparison to determine how the force produced during stretch differed
473 between myofibril groups. Significance was determined at 0.05 and used for all analyses.

474 **ACKNOWLEDGEMENTS**

475 The authors would like to acknowledge Jenna Monroy, Rene Fuqua and Uzma Tahir
476 from Northern Arizona University for their assistance in *mdm* tissue collection. In addition, the
477 authors would like to thank Scott Sibole and Venus Joumaa, University of Calgary, for
478 discussions which contributed to the final version of this manuscript. The nanofabricated
479 cantilevers used for force measurements were built by us at the NanoScale Facility of Cornell
480 University (Ithaca, NY), which is supported by the National Science Foundation.

481 **FUNDING**

482 This research was supported by the Canada Research Chair Program, The Killam
483 Foundation, Canadian Institutes of Health Research (CIHR), the Natural Sciences and

484 Engineering Research Council of Canada (NSERC), the National Science Foundation [NSF IOS
485 1025806] and the Austrian Science Fund [(FWF):T478-N13].

486 **DISCLOSURES**

487 No conflicts of interest, financial or otherwise, are declared by the authors.

488 **AUTHOR CONTRIBUTIONS**

489 Krysta Powers - data collection, analysis, paper preparation; Gudrun Schappacher-Tilp-
490 modeling; Azim Jinha - analysis, programming, editing; Tim Leonard – conception,
491 experimental design, editing; Kiisa Nishikawa - conceptual development, interpretation and
492 editing; Walter Herzog - experimental design, conceptual development, interpretation and final
493 editing.

494

495 **FIGURE CAPTIONS**

496 **Fig 1. Schematic representation of a sarcomere including thick, thin and titin filaments.**

497 The thick and thin filaments are the main contractile proteins. A-band titin runs the length of the
498 thick filament and is mainly structural. I-band titin is attached to the thin filament at the Z-disc
499 and contains titin's extensible spring segments. The proximal Ig, N2A, PEVK and distal Ig
500 domains of titin can extend during sarcomere stretch. Extension of the PEVK domain is the main
501 source of titin-based force.

502 **Fig. 2. Experimental set-up.** A single myofibril is attached to a glass needle used to manipulate
503 the length of the myofibril, and a cantilever used to measure the force produced by the myofibril.

504 **Fig. 3. Force and sarcomere length traces.** Force traces (A) in $\text{nN}/\mu\text{m}^2$ and individual
505 sarcomere lengths (B) from exemplary non-activated (blue) and activated (red) myofibrils. The
506 initiation of activation and duration of stretch are denoted by the vertical dotted lines. The force
507 (A) of activated myofibrils (red) remains higher than the force of the non-activated myofibrils
508 (blue) for the duration of stretch and following force relaxation to a steady-state. Individual
509 sarcomeres lengths (B) are non-uniform, however all measured sarcomeres are stretched beyond
510 filament overlap (gray area) during the implemented stretch.

511 **Fig. 4. A comparison of myofibril force-length curves from experimental conditions.** Force
512 normalized to myofibril cross-sectional area ($\text{nN}/\mu\text{m}^2$) \pm s.e.m. as a function of average
513 sarcomere length (μm). Myofibrils were stretched from an average initial sarcomere length of 2.5
514 μm to an average final sarcomere length of 6.0 μm . The loss of filament overlap is designated by
515 the dotted line. Myofibrils were stretched in a Ca^{2+} -rich activation solution (active, diamonds),
516 in activation solution with BDM, a cross-bridge inhibitor (BDM, squares), in activation solution
517 following chemical depletion of troponin-C (TnC-X, triangles), and in a low Ca^{2+} relaxing
518 solution (passive, circles). Activated myofibrils generated significantly more force than BDM,
519 TnC-X, and Passive myofibrils at all sarcomere lengths both within and beyond the region of
520 filament overlap ($p < 0.01$). BDM and TnC-X myofibrils generated significantly more force than
521 passive myofibrils at average sarcomere lengths of 3.5 - 6.0 μm ($p < 0.01$).

522 **Fig. 5. Predicted force-sarcomere length relationships from simulated data.** The predicted
523 titin-based force (grayed region) of actively stretched skeletal sarcomeres with N2A thin-

524 filament binding (black diamonds) exceeds predicted titin-based forces of actively stretched
525 sarcomeres without N2A thin-filament binding (gray diamonds) and predicted forces of
526 passively stretched sarcomeres (open circles). Predicted force of actively stretched sarcomeres in
527 the absence of N2A thin-filament binding is nearly diminished, with a small increase in predicted
528 force from passively stretched sarcomeres which can be attributed to calcium stiffening of titin's
529 PEVK and Ig domains.

530 **Fig 6. Proposed mechanism by which titin-based force is enhanced in the half sarcomere.**

531 The mechanism proposed occurs at the initiation of cross-bridge cycling when titin reversibly
532 binds to the thin filament at the N2A segment. This binding would significantly reduce the
533 available spring length of the passive titin spring (top panel, L_p). Thus, during Ca^{2+} - activation
534 and cross-bridge cycling the active titin spring length (bottom panel, L_a) would be much shorter
535 and stiffer, if the proposed mechanism is correct. If the sarcomere was stretched with an active
536 spring length of L_a rather than L_p , the passive force in the top panel half sarcomere would be
537 substantially less than that for the bottom panel half sarcomere even for stretches of identical
538 magnitudes.

539 **Fig. 7. Pilot data comparing force-length curves from active and passively stretched *mdm***

540 **myofibrils.** Force normalized to myofibril cross-sectional area ($nN/\mu m^2$) as a function of average
541 sarcomere length (μm) for a single active (diamond) and passive (circle) *mdm* myofibril.

542 Myofibrils were stretched from an average initial sarcomere length of $2.5 \mu m$ to an average final
543 sarcomere length of $6.0 \mu m$. The loss of filament overlap is designated by the dotted line. The
544 force of activated *mdm* myofibrils (triangle) remains higher than the force of the non-activated
545 *mdm* myofibrils (blue) for the duration of stretch. Titin-based force was increased during active
546 stretch, but to a lesser extent than in actively stretched wild-type myofibrils (Fig. 3).

547

548 REFERENCES

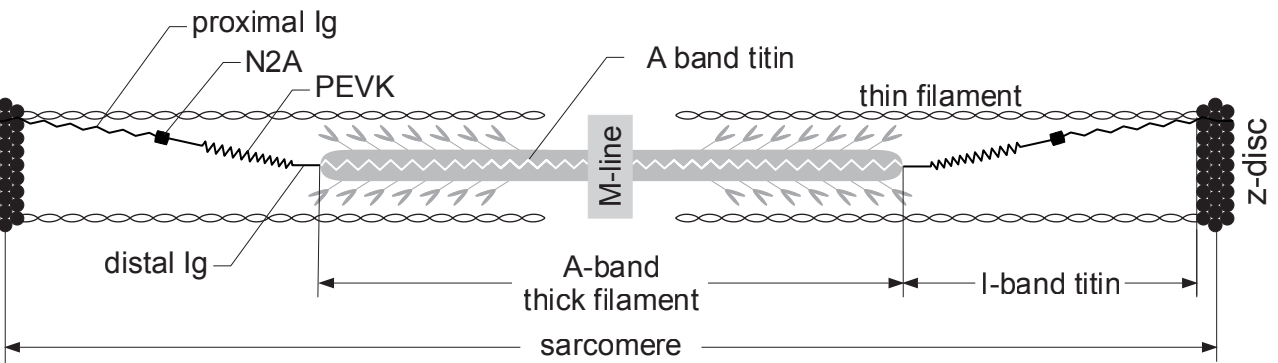
- 549 **Abbot, B. C. and Aubert, X. M.** (1952). The force exerted by active striated muscle during and
550 after change of length. *J. Physiol.* **117**, 77–86.
- 551 **Alegre-Cebollada, J., Kosuri, P., Giganti, D., Eckels, E., Rivas-Pardo, J. A., Hamdani, N.,**
552 **Warren, C. M., Solaro, R. J., Linke, W. A. and Fernández, J. M.** (2014). S-
553 Glutathionylation of Cryptic Cysteines Enhances Titin Elasticity by Blocking Protein
554 Folding. *Cell* **156**, 1235–1246.
- 555 **Bang, M.-L., Caremani, M., Brunello, E., Littlefield, R., Lieber, R. L., Chen, J., Lombardi,**
556 **V. and Linari, M.** (2009). Nebulin plays a direct role in promoting strong actin-myosin
557 interactions. *FASEB J.* **23**, 4117–4125.
- 558 **Bianco, P., Nagy, A., Kengyel, A., Szatmári, D., Mártonfalvi, Z., Huber, T. and**
559 **Kellermayer, M. S. Z.** (2007). Interaction forces between F-actin and titin PEVK
560 domain measured with optical tweezers. *Biophys. J.* **93**, 2102–2109.
- 561 **Burkholder, T. J. and Lieber, R. L.** (2001). Sarcomere length operating range of vertebrate
562 muscles during movement. *J. Exp. Biol.* **204**, 1529–1536.
- 563 **Campbell, K. S. and Moss, R. L.** (2002). History-dependent mechanical properties of
564 permeabilized rat soleus muscle fibers. *Biophys. J.* **82**, 929–943.
- 565 **DuVall, M. M., Gifford, J. L., Amrein, M. and Herzog, W.** (2013). Altered mechanical
566 properties of titin immunoglobulin domain 27 in the presence of calcium. *Eur. Biophys.*
567 *J. EBJ* **42**, 301–307.
- 568 **Edman, K. A., Elzinga, G. and Noble, M. I.** (1978). Enhancement of mechanical performance
569 by stretch during tetanic contractions of vertebrate skeletal muscle fibres. *J. Physiol.* **281**,
570 139–155.
- 571 **Edman, K. A., Elzinga, G. and Noble, M. I.** (1982). Residual force enhancement after stretch
572 of contracting frog single muscle fibers. *J. Gen. Physiol.* **80**, 769–784.
- 573 **Forcinito, M., Epstein, M. and Herzog, W.** (1998). Can a rheological muscle model predict
574 force depression/enhancement? *J. Biomech.* **31**, 1093–1099.
- 575 **Garvey, S. M., Rajan, C., Lerner, A. P., Frankel, W. N. and Cox, G. A.** (2002). The muscular
576 dystrophy with myositis (mdm) mouse mutation disrupts a skeletal muscle-specific
577 domain of titin. *Genomics* **79**, 146–149.
- 578 **Gautel, M. and Goulding, D.** (1996). A molecular map of titin/connectin elasticity reveals two
579 different mechanisms acting in series. *FEBS Lett.* **385**, 11–14.
- 580 **Gordon, A. M., Huxley, A. F. and Julian, F. J.** (1966). The variation in isometric tension with
581 sarcomere length in vertebrate muscle fibres. *J. Physiol.* **184**, 170–192.

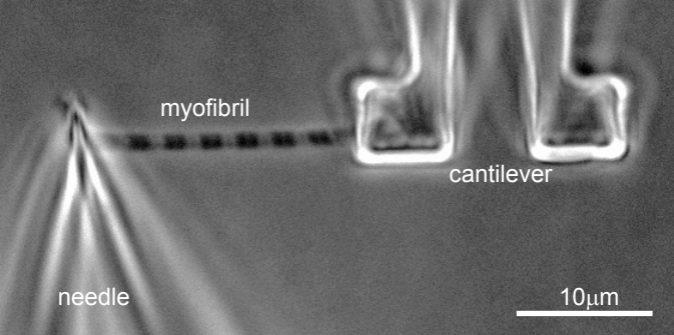
- 582 **Granzier, H. L.** (2010). Activation and stretch-induced passive force enhancement--are you
583 pulling my chain? Focus on "Regulation of muscle force in the absence of actin-myosin-
584 based cross-bridge interaction." *Am. J. Physiol. Cell Physiol.* **299**, C11–13.
- 585 **Granzier, H. L. and Irving, T. C.** (1995). Passive tension in cardiac muscle: contribution of
586 collagen, titin, microtubules, and intermediate filaments. *Biophys. J.* **68**, 1027–1044.
- 587 **Granzier, H. L. and Labeit, S.** (2004). The giant protein titin: a major player in myocardial
588 mechanics, signaling, and disease. *Circ. Res.* **94**, 284–295.
- 589 **Gregorio, C. C., Granzier, H., Sorimachi, H. and Labeit, S.** (1999). Muscle assembly: a
590 titanic achievement? *Curr. Opin. Cell Biol.* **11**, 18–25.
- 591 **Herzog, W. and Leonard, T. R.** (2002). Force enhancement following stretching of skeletal
592 muscle: a new mechanism. *J. Exp. Biol.* **205**, 1275–1283.
- 593 **Herzog, W., Kamal, S. and Clarke, H. D.** (1992). Myofilament lengths of cat skeletal muscle:
594 theoretical considerations and functional implications. *J. Biomech.* **25**, 945–948.
- 595 **Herzog, W., Lee, E. J. and Rassier, D. E.** (2006). Residual force enhancement in skeletal
596 muscle. *J. Physiol.* **574**, 635–642.
- 597 **Herzog, W., Duvall, M. and Leonard, T. R.** (2012a). Molecular mechanisms of muscle force
598 regulation: a role for titin? *Exerc. Sport Sci. Rev.* **40**, 50–57.
- 599 **Herzog, J. A., Leonard, T. R., Jinha, A. and Herzog, W.** (2012b). Are titin properties reflected
600 in single myofibrils? *J. Biomech.* **45**, 1893–1899.
- 601 **Herzog, W., Leonard, T., Joumaa, V., DuVall, M. and Panchangam, A.** (2012c). The three
602 filament model of skeletal muscle stability and force production. *Mol. Cell. Biomech.*
603 *MCB* **9**, 175–191.
- 604 **Hidalgo, C., Hudson, B., Bogomolovas, J., Zhu, Y., Anderson, B., Greaser, M., Labeit, S.**
605 **and Granzier, H.** (2009). PKC phosphorylation of titin's PEVK element: a novel and
606 conserved pathway for modulating myocardial stiffness. *Circ. Res.* **105**, 631–638, 17 p
607 following 638.
- 608 **Horowitz, R. and Podolsky, R. J.** (1987). The positional stability of thick filaments in activated
609 skeletal muscle depends on sarcomere length: evidence for the role of titin filaments. *J.*
610 *Cell Biol.* **105**, 2217–2223.
- 611 **Huebsch, K. A., Kudryashova, E., Wooley, C. M., Sher, R. B., Seburn, K. L., Spencer, M. J.**
612 **and Cox, G. A.** (2005). Mdm muscular dystrophy: interactions with calpain 3 and a
613 novel functional role for titin's N2A domain. *Hum. Mol. Genet.* **14**, 2801–2811.
- 614 **Huxley, A. F.** (1957). Muscle structure and theories of contraction. *Prog. Biophys. Biophys.*
615 *Chem.* **7**, 255–318.

- 616 **Huxley, A. F. and Niedergerke, R.** (1954). Structural changes in muscle during contraction;
617 interference microscopy of living muscle fibres. *Nature* **173**, 971–973.
- 618 **Huxley, A. F. and Simmons, R. M.** (1971). Proposed mechanism of force generation in striated
619 muscle. *Nature* **233**, 533–538.
- 620 **Joumaa, V., Rassier, D. E., Leonard, T. R. and Herzog, W.** (2008). The origin of passive
621 force enhancement in skeletal muscle. *Am. J. Physiol. Cell Physiol.* **294**, C74–78.
- 622 **Kellermayer, M. S. and Granzier, H. L.** (1996). Calcium-dependent inhibition of in vitro thin-
623 filament motility by native titin. *FEBS Lett.* **380**, 281–286.
- 624 **Kötter, S., Unger, A., Hamdani, N., Lang, P., Vorgerd, M., Nagel-Steger, L. and Linke, W.**
625 **A.** (2014). Human myocytes are protected from titin aggregation-induced stiffening by
626 small heat shock proteins. *J. Cell Biol.* **204**, 187–202.
- 627 **Krüger, M., Kötter, S., Grützner, A., Lang, P., Andresen, C., Redfield, M. M., Butt, E., dos**
628 **Remedios, C. G. and Linke, W. A.** (2009). Protein kinase G modulates human
629 myocardial passive stiffness by phosphorylation of the titin springs. *Circ. Res.* **104**, 87–
630 94.
- 631 **Labeit, D., Watanabe, K., Witt, C., Fujita, H., Wu, Y., Lahmers, S., Funck, T., Labeit, S.**
632 **and Granzier, H.** (2003). Calcium-dependent molecular spring elements in the giant
633 protein titin. *Proc. Natl. Acad. Sci. U. S. A.* **100**, 13716–13721.
- 634 **Leonard, T. R. and Herzog, W.** (2010). Regulation of muscle force in the absence of actin-
635 myosin-based cross-bridge interaction. *Am. J. Physiol. Cell Physiol.* **299**, C14–20.
- 636 **Leonard, T. R., DuVall, M. and Herzog, W.** (2010). Force enhancement following stretch in a
637 single sarcomere. *Am. J. Physiol. Cell Physiol.* **299**, C1398–1401.
- 638 **Linke, W. A., Stockmeier, M. R., Ivemeyer, M., Hossler, H. and Mundel, P.** (1998).
639 Characterizing titin's I-band Ig domain region as an entropic spring. *J. Cell Sci.* **111** (Pt
640 **11**), 1567–1574.
- 641 **Linke, W. A., Kulke, M., Li, H., Fujita-Becker, S., Neagoe, C., Manstein, D. J., Gautel, M.**
642 **and Fernandez, J. M.** (2002). PEVK domain of titin: an entropic spring with actin-
643 binding properties. *J. Struct. Biol.* **137**, 194–205.
- 644 **Llewellyn, M. E., Barretto, R. P. J., Delp, S. L. and Schnitzer, M. J.** (2008). Minimally
645 invasive high-speed imaging of sarcomere contractile dynamics in mice and humans.
646 *Nature* **454**, 784–788.
- 647 **Monroy, J. A., Lappin, A. K. and Nishikawa, K. C.** (2007). Elastic properties of active
648 muscle--on the rebound? *Exerc. Sport Sci. Rev.* **35**, 174–179.
- 649 **Monroy, J. A., Powers, K. L., Gilmore, L. A., Uyeno, T. A., Lindstedt, S. L. and Nishikawa,**
650 **K. C.** (2012). What is the role of titin in active muscle? *Exerc. Sport Sci. Rev.* **40**, 73–78.

- 651 **Morgan, D. L.** (1994). An explanation for residual increased tension in striated muscle after
652 stretch during contraction. *Exp. Physiol.* **79**, 831–838.
- 653 **Moss, R. L., Giulian, G. G. and Greaser, M. L.** (1985). The effects of partial extraction of TnC
654 upon the tension-pCa relationship in rabbit skinned skeletal muscle fibers. *J. Gen.*
655 *Physiol.* **86**, 585–600.
- 656 **Nishikawa, K. C., Monroy, J. A., Uyeno, T. E., Yeo, S. H., Pai, D. K. and Lindstedt, S. L.**
657 (2012). Is titin a “winding filament”? A new twist on muscle contraction. *Proc. Biol. Sci.*
658 **279**, 981–990.
- 659 **Page, S. G. and Huxley, H. E.** (1963). Filament lengths in striated muscle. *J. Cell Biol.* **19**, 369–
660 390.
- 661 **Panchangam, A. and Herzog, W.** (2011). Sarcomere overextension reduces stretch-induced
662 tension loss in myofibrils of rabbit psoas. *J. Biomech.* **44**, 2144–2149.
- 663 **Panchangam, A. and Herzog, W.** (2012). Overextended sarcomeres regain filament overlap
664 following stretch. *J. Biomech.* **45**, 2387–2391.
- 665 **Piazzesi, G. and Lombardi, V.** (1995). A cross-bridge model that is able to explain mechanical
666 and energetic properties of shortening muscle. *Biophys. J.* **68**, 1966–1979.
- 667 **Prado, L. G., Makarenko, I., Andresen, C., Krüger, M., Opitz, C. A. and Linke, W. A.**
668 (2005). Isoform diversity of giant proteins in relation to passive and active contractile
669 properties of rabbit skeletal muscles. *J. Gen. Physiol.* **126**, 461–480.
- 670 **Rassier, D. E.** (2012). Residual force enhancement in skeletal muscles: one sarcomere after the
671 other. *J. Muscle Res. Cell Motil.* **33**, 155–165.
- 672 **Rayment, I., Holden, H. M., Whittaker, M., Yohn, C. B., Lorenz, M., Holmes, K. C. and**
673 **Milligan, R. A.** (1993). Structure of the actin-myosin complex and its implications for
674 muscle contraction. *Science* **261**, 58–65.
- 675 **Schappacher-Tilp, G., Leonard, T., Desch, G. and Herzog, W.** (2014). A Novel Three-
676 Filament Model of Force Generation in Skeletal Muscles.
- 677 **Tatsumi, R., Maeda, K., Hattori, A. and Takahashi, K.** (2001). Calcium binding to an elastic
678 portion of connectin/titin filaments. *J. Muscle Res. Cell Motil.* **22**, 149–162.
- 679 **Tesi, C., Colomo, F., Piroddi, N. and Poggesi, C.** (2002). Characterization of the cross-bridge
680 force-generating step using inorganic phosphate and BDM in myofibrils from rabbit
681 skeletal muscles. *J. Physiol.* **541**, 187–199.
- 682 **Ting, L. Y. M., Minozzo, F. and Rassier, D. E.** (2012). Calcium Dependence of Titin-
683 Regulated Passive Forces in Skeletal Muscle Fibers. *Biophys. J.* **102**, 154a.

- 684 **Wang, K., McCarter, R., Wright, J., Beverly, J. and Ramirez-Mitchell, R.** (1991).
685 Regulation of skeletal muscle stiffness and elasticity by titin isoforms: a test of the
686 segmental extension model of resting tension. *Proc. Natl. Acad. Sci. U. S. A.* **88**, 7101–
687 7105.
- 688 **Wang, K., McCarter, R., Wright, J., Beverly, J. and Ramirez-Mitchell, R.** (1993).
689 Viscoelasticity of the sarcomere matrix of skeletal muscles. The titin-myosin composite
690 filament is a dual-stage molecular spring. *Biophys. J.* **64**, 1161–1177.
- 691 **Yamasaki, R., Berri, M., Wu, Y., Trombitás, K., McNabb, M., Kellermayer, M. S., Witt, C.,**
692 **Labeit, D., Labeit, S., Greaser, M., et al.** (2001). Titin-actin interaction in mouse
693 myocardium: passive tension modulation and its regulation by calcium/S100A1. *Biophys.*
694 *J.* **81**, 2297–2313.
- 695 **Yang, P., Tameyasu, T. and Pollack, G. H.** (1998). Stepwise dynamics of connecting filaments
696 measured in single myofibrillar sarcomeres. *Biophys. J.* **74**, 1473–1483.
- 697





myofibril

cantilever

needle

$10\mu\text{m}$

